A Measurement of the B_s^0 Lifetime using Reconstructed D_s^- Mesons

The OPAL Collaboration

Abstract

We report a measurement of the B_s^0 meson lifetime from $B_s^0 \rightarrow D_s^- X$ decays, where D_s^- mesons are reconstructed in the $D_s^- \rightarrow \phi\pi^-$ and $D_s^- \rightarrow K^{*0}K^-$ decay channels. From approximately 3.7 million hadronic Z^0 decays recorded by the OPAL detector at LEP a sample is selected containing 911 ± 83 candidates, of which 519 ± 136 are estimated to be from B_s^0 meson decays. Fitting the distribution of the distance from the beam spot to the decay vertex of the D_s^- candidates with an unbinned likelihood function we measure

$$\tau(B_s^0) = 1.72^{+0.20+0.18}_{-0.19-0.17}\,\text{ps},$$

where the errors are statistical and systematic, respectively.

(To be submitted to Zeitschrift für Physik)

K. Ackerstaff[8], G. Alexander[23], J. Allison[16], N. Altekamp[5], K.J. Anderson[9], S. Anderson[12],

S. Arcelli[2], S. Asai[24], D. Axen[29], G. Azuelos[18,a], A.H. Ball[17], E. Barberio[8], T. Barillari[2],

R.J. Barlow[16], R. Bartoldus[3], J.R. Batley[5], S. Baumann[3], J. Bechtluft[14], C. Beeston[16], T. Behnke[8],

A.N. Bell[1], K.W. Bell[20], G. Bella[23], S. Bentvelsen[8], S. Bethke[14], O. Biebel[14], A. Biguzzi[5],

S.D. Bird[16], V. Blobel[27], I.J. Bloodworth[1], J.E. Bloomer[1], M. Bobinski[10], P. Bock[11], D. Bonacorsi[2],

M. Boutemeur[34], B.T. Bouwens[12], S. Braibant[12], L. Brigliadori[2], R.M. Brown[20], H.J. Burckhart[8],

C. Burgard[8], R. Bürgin[10], P. Capiluppi[2], R.K. Carnegie[6], A.A. Carter[13], J.R. Carter[5],

C.Y. Chang[17], D.G. Charlton[1,b], D. Chrisman[4], P.E.L. Clarke[15], I. Cohen[23], J.E. Conboy[15],

O.C. Cooke[8], M. Cuffiani[2], S. Dado[22], C. Dallapiccola[17], G.M. Dallavalle[2], R. Davis[30], S. De Jong[12],

L.A. del Pozo[4], K. Desch[3], B. Dienes[33,d], M.S. Dixit[7], E. do Couto e Silva[12], M. Doucet[18],

E. Duchovni[26], G. Duckeck[34], I.P. Duerdoth[16], D. Eatough[16], J.E.G. Edwards[16], P.G. Estabrooks[6],

H.G. Evans[9], M. Evans[13], T. Geralis[20], G. Giacomelli[2], P. Giacomelli[4], R. Giacomelli[2], V. Gibson[5],

W.R. Gibson[13], D.M. Gingrich[30,a], D. Glenzinski[9], J. Goldberg[22], M.J. Goodrick[5], W. Gorn[4],

C. Grandi[2], E. Gross[26], J. Grunhaus[23], M. Gruwé[8], C. Hajdu[32], G.G. Hanson[12], M. Hansroul[8],

M. Hapke[13], C.K. Hargrove[7], P.A. Hart[9], C. Hartmann[3], M. Hauschild[8], C.M. Hawkes[5],

R. Hawkings[27], R.J. Hemingway[6], M. Herndon[17], G. Herten[10], R.D. Heuer[8], M.D. Hildreth[8],

J.C. Hill[5], S.J. Hillier[1], P.R. Hobson[25], R.J. Homer[1], A.K. Honma[28,a], D. Horváth[32,c],

K.R. Hossain[30], R. Howard[29], P. Hüntemeyer[27], D.E. Hutchcroft[5], P. Igo-Kemenes[11], D.C. Imrie[25],

M.R. Ingram[16], K. Ishii[24], A. Jawahery[17], P.W. Jeffreys[20], H. Jeremie[18], M. Jimack[1], A. Joly[18],

C.R. Jones[5], G. Jones[16], M. Jones[6], U. Jost[11], P. Jovanovic[1], T.R. Junk[8], D. Karlen[6],

V. Kartvelishvili[16], K. Kawagoe[24], T. Kawamoto[24], P.I. Kayal[30], R.K. Keeler[28], R.G. Kellogg[17],

B.W. Kennedy[20], J. Kirk[29], A. Klier[26], S. Kluth[8], T. Kobayashi[24], M. Kobel[10], D.S. Koetke[6],

T.P. Kokott[3], M. Kolrep[10], S. Komamiya[24], T. Kress[11], P. Krieger[6], J. von Krogh[11], P. Kyberd[13],

G.D. Lafferty[16], R. Lahmann[17], W.P. Lai[19], D. Lanske[14], J. Lauber[15], S.R. Lautenschlager[31],

J.G. Layter[4], D. Lazic[22], A.M. Lee[31], E. Lefebvre[18], D. Lellouch[26], J. Letts[12], L. Levinson[26],

S.L. Lloyd[13], F.K. Loebinger[16], G.D. Long[28], M.J. Losty[7], J. Ludwig[10], A. Macchiolo[2],

A. Macpherson[30], M. Mannelli[8], S. Marcellini[2], C. Markus[3], A.J. Martin[13], J.P. Martin[18],

G. Martinez[17], T. Mashimo[24], P. Mättig[3], W.J. McDonald[30], J. McKenna[29], E.A. Mckigney[15],

T.J. McMahon[1], R.A. McPherson[8], F. Meijers[8], S. Menke[3], F.S. Merritt[9], H. Mes[7], J. Meyer[27],

A. Michelini[2], G. Mikenberg[26], D.J. Miller[15], A. Mincer[22,e], R. Mir[26], W. Mohr[10], A. Montanari[2],

T. Mori[24], M. Morii[24], U. Müller[3], S. Mihara[24], K. Nagai[26], I. Nakamura[24], H.A. Neal[8], B. Nellen[3],

R. Nisius[8], S.W. O'Neale[1], F.G. Oakham[7], F. Odorici[2], H.O. Ogren[12], A. Oh[27], N.J. Oldershaw[16],

M.J. Oreglia[9], S. Orito[24], J. Pálinkás[33,d], G. Pásztor[32], J.R. Pater[16], G.N. Patrick[20], J. Patt[10],

M.J. Pearce[1], R. Perez-Ochoa8, S. Petzold[27], P. Pfeifenschneider[14], J.E. Pilcher[9], J. Pinfold[30],

D.E. Plane[8], P. Poffenberger[28], B. Poli[2], A. Posthaus[3], D.L. Rees[1], D. Rigby[1], S. Robertson[28],

S.A. Robins[22], N. Rodning[30], J.M. Roney[28], A. Rooke[15], E. Ros[8], A.M. Rossi[2], P. Routenburg[30],

Y. Rozen[22], K. Runge[10], O. Runolfsson[8], U. Ruppel[14], D.R. Rust[12], R. Rylko[25], K. Sachs[10],

T. Saeki[24], E.K.G. Sarkisyan[23], C. Sbarra[29], A.D. Schaile[34], O. Schaile[34], F. Scharf[3],

P. Scharff-Hansen[8], P. Schenk[34], J. Schieck[11], P. Schleper[11], B. Schmitt[8], S. Schmitt[11],

A. Schöning[8], M. Schröder[8], H.C. Schultz-Coulon[10], M. Schumacher[3], C. Schwick[8], W.G. Scott[20],

T.G. Shears[16], B.C. Shen[4], C.H. Shepherd-Themistocleous[8], P. Sherwood[15], G.P. Siroli[2],

A. Sittler[27], A. Skillman[15], A. Skuja[17], A.M. Smith[8], G.A. Snow[17], R. Sobie[28],

S. Söldner-Rembold[10], R.W. Springer[30], M. Sproston[20], K. Stephens[16], J. Steuerer[27],

B. Stockhausen[3], K. Stoll[10], D. Strom[19], P. Szymanski[20], R. Tafirout[18], S.D. Talbot[1], S. Tanaka[24],

P. Taras[18], S. Tarem[22], R. Teuscher[8], M. Thiergen[10], M.A. Thomson[8], E. von Törne[3], S. Towers[6],

I. Trigger[18], Z. Trócsányi[33], E. Tsur[23], A.S. Turcot[9], M.F. Turner-Watson[8], P. Utzat[11], R. Van

Kooten[12], M. Verzocchi[10], P. Vikas[18], E.H. Vokurka[16], H. Voss[3], F. Wäckerle[10], A. Wagner[27],

C.P. Ward[5], D.R. Ward[5], P.M. Watkins[1], A.T. Watson[1], N.K. Watson[1], P.S. Wells[8], N. Wermes[3],

J.S. White[28], B. Wilkens[10], G.W. Wilson[27], J.A. Wilson[1], G. Wolf[26], T.R. Wyatt[16], S. Yamashita[24], G. Yekutieli[26], V. Zacek[18], D. Zer-Zion[8]

[1]School of Physics and Space Research, University of Birmingham, Birmingham B15 2TT, UK
[2]Dipartimento di Fisica dell' Università di Bologna and INFN, I-40126 Bologna, Italy
[3]Physikalisches Institut, Universität Bonn, D-53115 Bonn, Germany
[4]Department of Physics, University of California, Riverside CA 92521, USA
[5]Cavendish Laboratory, Cambridge CB3 0HE, UK
[6] Ottawa-Carleton Institute for Physics, Department of Physics, Carleton University, Ottawa, Ontario K1S 5B6, Canada
[7]Centre for Research in Particle Physics, Carleton University, Ottawa, Ontario K1S 5B6, Canada
[8]CERN, European Organisation for Particle Physics, CH-1211 Geneva 23, Switzerland
[9]Enrico Fermi Institute and Department of Physics, University of Chicago, Chicago IL 60637, USA
[10]Fakultät für Physik, Albert Ludwigs Universität, D-79104 Freiburg, Germany
[11]Physikalisches Institut, Universität Heidelberg, D-69120 Heidelberg, Germany
[12]Indiana University, Department of Physics, Swain Hall West 117, Bloomington IN 47405, USA
[13]Queen Mary and Westfield College, University of London, London E1 4NS, UK
[14]Technische Hochschule Aachen, III Physikalisches Institut, Sommerfeldstrasse 26-28, D-52056 Aachen, Germany
[15]University College London, London WC1E 6BT, UK
[16]Department of Physics, Schuster Laboratory, The University, Manchester M13 9PL, UK
[17]Department of Physics, University of Maryland, College Park, MD 20742, USA
[18]Laboratoire de Physique Nucléaire, Université de Montréal, Montréal, Quebec H3C 3J7, Canada
[19]University of Oregon, Department of Physics, Eugene OR 97403, USA
[20]Rutherford Appleton Laboratory, Chilton, Didcot, Oxfordshire OX11 0QX, UK
[22]Department of Physics, Technion-Israel Institute of Technology, Haifa 32000, Israel
[23]Department of Physics and Astronomy, Tel Aviv University, Tel Aviv 69978, Israel
[24]International Centre for Elementary Particle Physics and Department of Physics, University of Tokyo, Tokyo 113, and Kobe University, Kobe 657, Japan
[25]Brunel University, Uxbridge, Middlesex UB8 3PH, UK
[26]Particle Physics Department, Weizmann Institute of Science, Rehovot 76100, Israel
[27]Universität Hamburg/DESY, II Institut für Experimental Physik, Notkestrasse 85, D-22607 Hamburg, Germany
[28]University of Victoria, Department of Physics, P O Box 3055, Victoria BC V8W 3P6, Canada
[29]University of British Columbia, Department of Physics, Vancouver BC V6T 1Z1, Canada
[30]University of Alberta, Department of Physics, Edmonton AB T6G 2J1, Canada
[31]Duke University, Dept of Physics, Durham, NC 27708-0305, USA
[32]Research Institute for Particle and Nuclear Physics, H-1525 Budapest, P O Box 49, Hungary
[33]Institute of Nuclear Research, H-4001 Debrecen, P O Box 51, Hungary
[34]Ludwigs-Maximilians-Universität München, Sektion Physik, Am Coulombwall 1, D-85748 Garching, Germany
[a] and at TRIUMF, Vancouver, Canada V6T 2A3
[b] and Royal Society University Research Fellow
[c] and Institute of Nuclear Research, Debrecen, Hungary
[d] and Department of Experimental Physics, Lajos Kossuth University, Debrecen, Hungary
[e] and Department of Physics, New York University, NY 1003, USA

1   Introduction

The lifetimes of b-flavored hadrons are related to both the strength of the b quark coupling to c and u quarks, and to the dynamics of b hadron decay. The spectator model assumes that the light quarks in b and c hadrons do not affect the decay of the heavy quark, and thus predicts the lifetimes of all b-hadrons to be equal. For charm hadrons this prediction is inaccurate; the measured D^+ lifetime is approximately 2.5 times that of the D^0 and more than twice that of the D_s^- [1]. More sophisticated models predict that the differences among b-hadron lifetimes should be much smaller than those in the charm system, because of the larger mass of the b quark [2, 3, 4]. Bigi et al. [3] predict a difference in lifetime between the B^+ and B^0 meson of several percent, and between the B_s^0 and B^0 mesons of about 1%. Although some assumptions in reference [3] have been questioned by Neubert and Sachrajda [4], there is agreement that the models predict a difference between the B_s^0 and B^0 lifetimes of the order of $\pm 1\%$.

The first measurements of the B_s^0 lifetime [5, 6] were made using correlated D_s^--lepton pairs that primarily result from the semileptonic decay of the B_s^0. However, the small B_s^0 semileptonic branching ratio limits the statistical power of this channel. More inclusive techniques can be used to circumvent this limitation.

We present a new measurement of the lifetime of the B_s^0 meson in which only the D_s^- mesons are reconstructed. The two decay channels used are:[1]

$$
\begin{array}{ll}
B_s^0 \to D_s^- \, X & B_s^0 \to D_s^- \, X \\
\quad \hookrightarrow \; K^{*0} \, K^- & \quad \hookrightarrow \; \phi \, \pi^- \\
\quad\quad \hookrightarrow \; K^+ \, \pi^- & \quad\quad \hookrightarrow \; K^+ \, K^- .
\end{array}
\qquad \text{and}
$$

The B_s^0 meson is not the only source of D_s^- mesons. Significant numbers of D_s^- mesons are produced in the decays of other b-hadrons as well as in $Z^0 \to c\bar{c}$ events. The level and shape of this background is evaluated using Monte Carlo data and measured branching fractions. The background from random tracks combination is evaluated using the side band technique.

To measure the B_s^0 lifetime, we reconstruct the decay vertex of the D_s^- and determine the distance from the beam spot to this point. For D_s^- mesons that result from the decay of b-hadrons, this "decay length" has contributions both from the b-hadron and D_s^- decay lengths. The bias arising from the angle between the B_s^0 meson and the D_s^- meson direction is very small and is not affecting the result of this analysis. An unbinned maximum likelihood fit is performed using the reconstructed decay lengths, their errors and the D_s^- momentum to extract the mean B_s^0 lifetime. The following sections describe the OPAL detector, the selection of D_s^- candidates, the vertex topology of the events, the determination of the B_s^0 decay length, the estimation of the B_s^0 energy, the lifetime fit, the results, and the systematic errors.

---

[1]Charge conjugate modes are always implied. Also, unless otherwise noted, K and π always refer to charged particles.

2   The OPAL Detector

The OPAL detector is described in reference [7]. The central tracking system is composed of a silicon microvertex detector, a precision vertex drift chamber and a large volume jet chamber surrounded by a set of chambers to measure the z-coordinate of tracks (z-chambers)[2]. These detectors are located inside a solenoid. The detectors outside the solenoid consist of a time-of-flight scintillator array and a lead glass electromagnetic calorimeter with a presampler, followed by a hadron calorimeter consisting of the instrumented return yoke of the magnet, and several layers of muon chambers. Charged particle types are identified by their specific energy loss, dE/dx, in the jet chamber. Further information on the performance of the tracking and dE/dx measurements can be found in reference [8].

3 D_s^- Candidate Selection

This analysis uses data collected during the 1991–1995 LEP running periods at center-of-mass energies within $\pm 3\,\mathrm{GeV}$ of the Z^0 mass. After the standard hadronic event selection [9] and detector performance requirements, a sample of 3.7 million events is selected. Charged tracks and electromagnetic clusters not associated with a charged track are grouped into jets using the JADE E0 recombination scheme [10] with a y_{cut} value of 0.04. Tracks from identified secondary vertices, Λ and K_S^0 decays or γ conversions, are excluded from the B_s^0 candidate selection.

Simulated event samples were generated using the JETSET 7.4 Monte Carlo program [11], together with a program to simulate the response of the OPAL detector [12]. The Monte Carlo sample includes approximately 4 million simulated multihadronic Z^0 decays and one million $Z^0 \to b\bar{b}$ decays (the equivalent of about 4.5 million multihadronic decays). In addition, three special Monte Carlo samples were generated in which each event contains at least one D_s^- decaying in the channels of interest. The parameter optimisation used in this simulation is described in [11]. For each of the following decay channels, 20000 events were generated: $D_s^- \to D_s^- X$, D_s^- from b-hadrons other than D_s^- decays and D_s^- from $Z^0 \to c\bar{c}$.

3.1 $D_s^- \to K^+ K^- \pi^-$ selection

The D_s^- meson is reconstructed in the decay chains $D_s^- \to K^{*0} K^-$ in which the K^{*0} decays into a $K^+ \pi^-$, and $D_s^- \to \phi \pi^-$ where the ϕ subsequently decays into $K^+ K^-$.

Tracks forming the D_s^- candidates are required to be in the same jet and to have the appropriate charge combination. At least two of the three candidate tracks are required to have good θ measurements either from the z-chambers or from a measurement of the track endpoint as it exits the main jet chamber. Similarly, to reject poorly reconstructed candidates, at least two of the three tracks are required to have hits in the silicon microvertex detector.

---

[2]The coordinate system is defined such that the z-axis follows the electron beam direction and the x-y plane is perpendicular to it with the x-axis lying horizontally. The polar angle θ is defined relative to the $+z$-axis, and the azimuthal angle ϕ is defined relative to the $+x$-axis.

To reduce the combinatorial background, the tracks forming the D_s^- are subject to particle identification requirements. For candidate pion tracks, the probability for the measured dE/dx value to be consistent with the pion hypothesis is required to be greater than 1%. For candidate kaon tracks, if the observed energy loss of a kaon candidate is less than the mean dE/dx expected for a kaon, the probability of consistency with the kaon hypothesis is required to be greater than 1%, and greater than 3% otherwise. If both kaon candidates have energy losses greater than the mean dE/dx expected for a kaon, the product of the two dE/dx probabilities is required to be greater than 0.02. These tighter requirements reduce the background from pion tracks, for which the mean dE/dx value is above that of kaons. Furthermore, one of the kaon candidates must satisfy a pion-rejection criterion by having an observed dE/dx less than that expected for a pion, and a probability of less than 10% that the dE/dx is consistent with a pion hypothesis.

For the $K^{*0}K^-$ mode, the invariant mass of the $K\pi$ combination is required to satisfy $0.865 < m_{K\pi} < 0.925\,\mathrm{GeV}$. In the $\phi\pi$ mode, the width of the K^+K^- peak is dominated by detector resolution and the K^+K^- invariant mass is required to satisfy $1.010 < m_{KK} < 1.030\,\mathrm{GeV}$. The momenta of the kaons are required to be greater than $2\,\mathrm{GeV}$ and that of the pion must exceed $1\,\mathrm{GeV}$.

To reduce further the $D^- \to K^{*0}\pi^-$ background in the $K^{*0}K^-$ mode, the kaon candidate originating directly from the D_s^- decay is subject to a tighter, 5%, dE/dx requirement. Also, in this mode both kaons must meet the pion-rejection criterion described above.

We require that the D_s^- momentum divided by the beam energy, $x_{D_s^-}$, is greater than 0.15 to reduce random track combinations, and less than 0.60 to reduce the D_s^- contribution from $Z^0 \to c\bar{c}$ events.

The differences between the angular distributions of D_s^- decays and those of combinatorial background are exploited to enhance the signal purity as follow. The D_s^- is a spin-0 meson and the final states of both decay modes consist of a spin-1 (ϕ or K^{*0}) meson and a spin-0 (π^- or K^-) meson. The D_s^- signal is expected to have no dependence on $\cos\theta_p$, where θ_p is the angle in the rest frame of the D_s^- between the spin-0 meson direction and the D_s^- direction in the lab frame. However, the $\cos\theta_p$ distribution of random combinations peaks in the forward and backward directions. It is therefore required that $|\cos\theta_p| < 0.8$ for both modes. The distribution of $\cos\theta_v$, the angle in the rest frame of the spin-1 meson between the direction of the final state kaon from the decay of the spin-1 meson and the D_s^- direction, is proportional to $\cos^2\theta_v$ for D_s^- decays. The $\cos\theta_v$ distribution of the random $K^+K^-\pi^-$ combinations in the data is, however, approximately uniform. Therefore it is required that $|\cos\theta_v| > 0.6\ (0.4)$ for the K^*K ($\phi\pi$) mode.

3.2 Decay length determination

The D_s^- decay vertex is reconstructed in the x-y plane by fitting the D_s^- candidate tracks to a vertex. To reject very poorly reconstructed vertices, the χ^2 of the vertex fit is required to be less than 10 (for 1 degree of freedom).

The beam spot position is measured using charged tracks in the opal data with a technique that follows any significant shifts in the position during a LEP fill [13]. The intrinsic width

of the beam spot in the y direction is about $8\,\mu$m. the width in the x direction is directly measured using $\mu^+\mu^-$ events and varies between $100\,\mu$m and $160\,\mu$m, depending on the LEP optics.

The distance from the D_s^- decay vertex to the beam spot is determined in the x-y plane. This distance is converted into three dimensions using the polar angle of the $K^+K^-\pi^-$ momentum vector. Typical decay length errors are about $300\,\mu$m, with only a small contribution coming from uncertainties in the position of the interaction point within the beam spot. Rejecting candidates with decay length errors greater than 3 mm helps to reduce the effects of poorly measured tracks.

3.3 D_s^- selection results

The $K^+K^-\pi^-$ invariant mass distribution for all candidates that pass the selection is shown in figure 1. A likelihood fit to the measured $K^+K^-\pi^-$ invariant mass of the D_s^- candidates is performed separately for the two decay channels. The $K^+K^-\pi^-$ mass distribution is parameterized as the sum of a quadratic term to account for random combinatorial background (which also is observed to describe accurately the background in the simulated data samples), a Gaussian function which describes the mass peak of the reconstructed D_s^- signal, and another Gaussian to account for a $D^- \to K^+K^-\pi^-$ contribution. This last term has a mean fixed to the D^- mass of 1869.3 MeV [1] and the width constrained to be the same as that of the D_s^- signal. This second Gaussian is included to avoid biasing the estimate of the combinatorial background. The results of this fit to the $K^+K^-\pi^-$ invariant mass spectra are shown in table 1. A total of 911 ± 83 D_s^- candidates are found.

source	$\phi\pi$	K^*K
number of D_s^- candidates	629 ± 64	282 ± 53
fitted D_s^- mass	$1.966 \pm 0.002\,\mathrm{GeV}$	$1.959 \pm 0.004\,\mathrm{GeV}$
fitted D_s^- sigma	$18 \pm 2\,\mathrm{MeV}$	$21 \pm 3\,\mathrm{MeV}$
background fraction	0.75	0.86
total χ^2 over 80 bins	90.0	80.0

Table 1: $K^+K^-\pi^-$ invariant mass spectra fitting results. The fitted mass is in agreement with the value of 1.9685 ± 0.0006MeV from [1]. The "background fraction" is defined as the fitted number of combinatorial background candidates divided by the total number of candidates within 2σ of the fitted D_s^- mass.

3.4 Composition of the D_s^- signal

The B_s^0 meson is not the only source of D_s^- mesons. Significant numbers of D_s^- mesons are produced in other b-hadron decays as well as in $Z^0 \to c\bar{c}$ events, collectively referred to as 'physics background'. In what follows, the contributions of these three components to the observed D_s^- spectra are estimated.

The fractions of D_s^- mesons produced from each of these sources are extracted using the results in reference [14]. The measured D_s^- production rates separated into flavour are

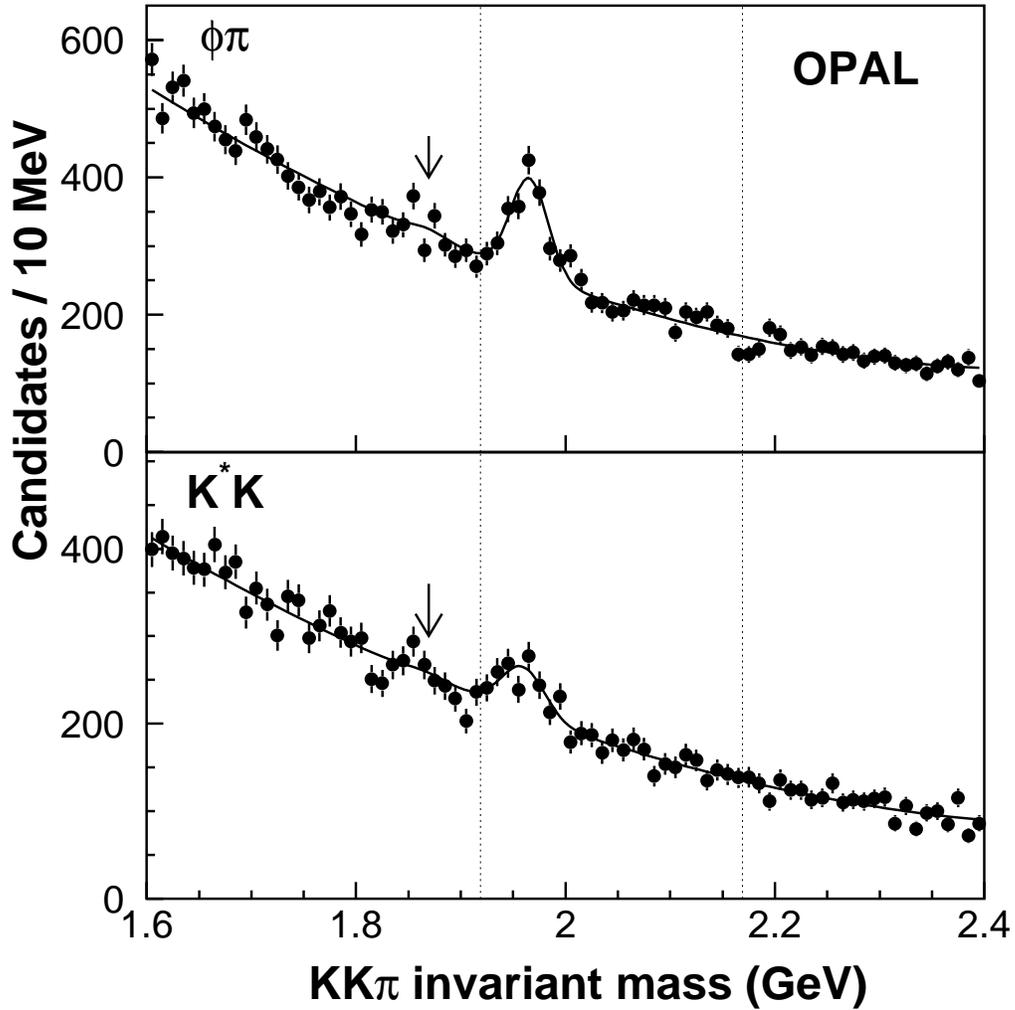Figure 1: Results of the standard selection. Top: $K^+K^-\pi^-$ invariant mass distribution for $\phi\pi$ combinations along with the fitted distribution. Bottom: $K^+K^-\pi^-$ invariant mass distribution for K^*K candidates, along with the fitted distribution. The dotted lines indicate the region within which candidates are used in the lifetime fit. The arrow indicates the D^- peak position.

$f_{\mathrm{b}} = \Gamma_{\mathrm{b\bar{b}}}/\Gamma_{\mathrm{had}} \cdot f(\mathrm{b} \to \mathrm{D_s^-}) \cdot \mathrm{Br}(\mathrm{D_s^-} \to \phi\pi^-) = (0.166 \pm 0.018 \pm 0.016)\%$ and $f_{\mathrm{c}} = \Gamma_{\mathrm{c\bar{c}}}/\Gamma_{\mathrm{had}} \cdot f(\mathrm{c} \to \mathrm{D_s^-}) \cdot \mathrm{Br}(\mathrm{D_s^-} \to \phi\pi^-) = (0.056 \pm 0.015 \pm 0.007)\%$. Thus, $f_{\mathrm{b}}/(f_{\mathrm{c}} + f_{\mathrm{b}}) = (75 \pm 9)\%$ of produced $\mathrm{D_s^-}$ mesons are from $\mathrm{Z^0} \to \mathrm{b\bar{b}}$ events and the remaining $(25 \pm 9)\%$ are from $\mathrm{Z^0} \to \mathrm{c\bar{c}}$ events.

The fraction of $\mathrm{D_s^-}$ mesons from b-hadrons in our signal is estimated using the following production rates: $f(\mathrm{b} \to \mathrm{B_s^0}) = 0.112^{+0.018}_{-0.019}$ [1] and $f(\mathrm{b} \to \mathrm{B}) = 0.378 \pm 0.022$ [1] (where 'B' is either $\mathrm{B^+}$ or $\mathrm{B^0}$). Assuming that b-baryons decay to $\mathrm{D_s^-}$ mesons with the same branching fractions as the non-strange b-mesons $(0.086 \pm 0.016$ [1]) and using the inclusive branching ratio of $\mathrm{B_s^0}$ to $\mathrm{D_s^-}$, measured to be 0.87 ± 0.31 [1], we estimate that $(56 \pm 11)\%$ of $\mathrm{D_s^-}$ mesons from b-hadron decay are from $\mathrm{B_s^0}$. Thus, $(42 \pm 10)\%$ of the $\mathrm{D_s^-}$ mesons come from $\mathrm{B_s^0}$ decays, $(33 \pm 9)\%$ come from other b-hadron decays and $(25 \pm 9)\%$ from $\mathrm{Z^0} \to \mathrm{c\bar{c}}$ events. Assuming the production rates of $\mathrm{B^+}$ and $\mathrm{B^0}$ are the same and that they have equal branching ratios to $\mathrm{D_s^-}$, each of these non-strange b-mesons accounts for $(14 \pm 4)\%$ of the $\mathrm{D_s^-}$ production with the remaining $(5 \pm 2)\%$ of $\mathrm{D_s^-}$ produced from b-baryons.

The special Monte Carlo samples described above were used to determine the contribution of each of these channels i the reconstructed sample. The ratio of the efficiency to reconstruct a $\mathrm{D_s^-}$ meson from b-hadron decay other than $\mathrm{B_s^0}$, divided by the efficiency to reconstruct a $\mathrm{D_s^-}$ meson from a $\mathrm{B_s^0}$ decay is 0.82 ± 0.02, where the error is due to the limited statistics of the simulated data samples. The principal reason that this ratio is less than unity is that the momentum spectrum of $\mathrm{D_s^-}$ mesons from the decay of b-hadrons other than $\mathrm{B_s^0}$ is softer than that of $\mathrm{D_s^-}$ mesons from $\mathrm{B_s^0}$ decay. The ratio of the efficiency to reconstruct a $\mathrm{D_s^-}$ meson from a $\mathrm{Z^0} \to \mathrm{c\bar{c}}$ event divided by the efficiency to reconstruct a $\mathrm{D_s^-}$ from a $\mathrm{B_s^0}$ decay is 0.67 ± 0.01. The upper cut on the scaled energy of the $\mathrm{D_s^-}$ ($x_{\mathrm{D_s^-}} < 0.6$) preferentially rejects $\mathrm{D_s^-}$ from $\mathrm{Z^0} \to \mathrm{c\bar{c}}$, which tend to have higher momentum. the sources of $\mathrm{D_s^-}$ production are summarized in table 2.

source	fraction of produced $\mathrm{D_s^-}$	fraction of reconstructed $\mathrm{D_s^-}$
$\mathrm{Z^0} \to \mathrm{c\bar{c}}$	25 ± 9	17 ± 6
$\mathrm{B^+}$	14 ± 4	11 ± 3
$\mathrm{B^0}$	14 ± 4	11 ± 3
b-baryons	5 ± 2	4 ± 2
$\mathrm{B_s^0}$	42 ± 10	57 ± 14

Table 2: Estimated $\mathrm{D_s^-}$ signal composition. The errors include those from the measured branching ratios and the statistical uncertainty from the Monte Carlo samples used to estimate the relative reconstruction efficiencies.

Monte Carlo events were used to study the background from events where the three $\mathrm{K^+K^-\pi^-}$ candidate tracks come either from the same fully reconstructed charm hadron for which a pion or a proton has been mis-identified as a kaon, or from a partially reconstructed charm hadron. The resulting $\mathrm{K^+K^-\pi^-}$ invariant mass distribution in the region around the $\mathrm{D_s^-}$ mass is similar to that of the combinatorial background. Such events are therefore, considered to contribute to the combinatorial background.

Since $(57 \pm 14)\%$ of the reconstructed $\mathrm{D_s^-}$ meson decays are calculated to be from $\mathrm{B_s^0}$ decays, 519 ± 136 $\mathrm{D_s^-}$ candidates are attributed to $\mathrm{B_s^0}$ decay from the 911 ± 83 candidates resulting from the fit to the $\mathrm{K^+K^-\pi^-}$ invariant spectra.

4   The B_s^0 Lifetime Fit

To extract the B_s^0 lifetime from the measured decay lengths, an unbinned maximum likelihood fit is performed using a function that accounts for both the D_s^- signal and the background components of the sample. In the part of the likelihood function describing events from b-hadron decays, the observed decay lengths depend on the B_s^0 lifetime.

The form of the likelihood function for the candidates in the D_s^- signal from B_s^0 decays is described in terms of the probability for observing a combined D_s^- and B_s^0 decay length, L^i, given a measurement error σ_L^i, the momenta of the D_s^- and B_s^0, and the mean lifetimes of these mesons.

The likelihood function has components which describe the different sources of D_s^- mesons in the signal and in the combinatorial background. This follows closely the method used in previous opal B_s^0 lifetime analyses [6].

The likelihood function which accounts for D_s^- mesons from B_s^0 decays is constructed as a convolution of two exponential functions to describe the D_s^- and B_s^0 decay lengths, convoluted with a function to describe the probability of having a particular B_s^0 momentum (p_{B_s}) and Gaussian functions to describe the measured decay length resolution. This can be expressed as:

$$\mathcal{L}_i^{B_s^0}(L^i \mid \tau_{B_s^0}, \sigma_L^i, p_{D_s}^i, s_1, s_2, f_2) =$$

$$\int_0^\infty \mathrm{d}l \int_0^{p_{B_s}(max)} \mathrm{d}p_{B_s}\, \mathcal{R}(L^i \mid l, \sigma_L^i, s_1, s_2, f_2)\, \mathcal{B}(p_{B_s} \mid p_{D_s}^i)\, \mathcal{P}(l \mid \tau_{B_s^0}, \tau_{D_s^-}, p_{B_s}, p_{D_s}^i) \qquad (1)$$

where $p_{B_s}(max) = 45\text{GeV}$ and $\mathcal{R}$ is given by

$$\mathcal{R}(L^i \mid l, \sigma_L^i, s_1, s_2, f_2) = (1 - f_2)\,\mathcal{G}(L^i \mid l, \sigma_L^i, s_1) + f_2\,\mathcal{G}(L^i \mid l, \sigma_L^i, s_2)\ . \qquad (2)$$

The function } is a Gaussian function which describes the probability to observe a decay length, L^i, given a true decay length l and the measurement uncertainty σ_L^i and scale factors on this error, s_1 and s_2. Two scale factors are employed to describe both the majority of tracks for which the measured decay length uncertainty is a good estimate and the small fraction, f_2, of mis-measured candidates in which the measured decay length uncertainty is an underestimate. The scale factors s_1 and s_2, as well as the fraction of mis-measured candidates, f_2, are free parameters in the lifetime fit. $\mathcal{B}$ is the probability of a particular B_s^0 momentum for an observed D_s^- momentum, p_{D_s}. This probability is determined from Monte Carlo events by forming distributions of the ratio p_{B_s}/p_{D_s}. Six such distributions are formed, depending on the value of p_{D_s}, since at higher values of p_{D_s} the range of potential values of p_{B_s} is more tightly constrained than for lower p_{D_s} candidates. $\mathcal{P}$ is the probability for the D_s^- to decay at a distance l from the e^+e^- interaction point, given B_s^0 and D_s^- lifetimes $\tau_{B_s^0}$ and $\tau_{D_s^-}$ and momenta p_{B_s} and $p_{D_s}^i$. This function is constructed as:

$$\mathcal{P}(l \mid \tau_{B_s^0}, p_{B_s}, p_{D_s}, s_1, s_2, f_2) = \frac{m_{D_s}}{\tau_{D_s^-} p_{D_s}} \frac{m_{B_s}}{\tau_{B_s^0} p_{B_s}} \int_0^l \exp\left[\frac{-l' \cdot m_{B_s}}{\tau_{B_s^0} p_{B_s}}\right] \exp\left[\frac{-(l - l') \cdot m_{D_s}}{\tau_{D_s^-} p_{D_s}}\right] \mathrm{d}l'$$
$$(3)$$

where $\tau_{B_s^0} p_{B_s}/m_{B_s}$ and $\tau_{D_s^-} p_{D_s}/m_{D_s}$ are the mean decay lengths for the given momenta (p_{B_s} and p_{D_s}) mean lifetimes ($\tau_{B_s^0}$ and $\tau_{D_s^-}$) and masses (m_{B_s} and m_{D_s}).

Similar functions are employed for the other D_s^- meson sources. For D_s^- mesons from other b-hadron decays (B^+, B^0 and b-baryons), the world average lifetime for each species of b-hadron [1] is used in the likelihood function and a slightly different boost function, $\mathcal{B}$, is employed. For D_s^- mesons produced in $Z^0 \to c\bar{c}$ events, the function $\mathcal{P}$ is a single exponential function with the decay constant $\tau_{D_s^-} p_{D_s}/m_{D_s}$. The total likelihood function containing the contributions for all sources of D_s^- mesons, is formed by combining the likelihood functions for each of the sources of D_s^- mesons with the fixed fractions listed in table 2.[3] This likelihood is written as:

$$\mathcal{L}_i^{D_s^-}(L^i \mid \tau_{B_s^0}, \sigma_L^i, p_{D_s}^i) = (1 - f_{c\bar{c}} - f_{B^+} - f_{B^0} - f_{\Lambda_b})\mathcal{L}_i^{B_s^0} + \\ f_{c\bar{c}} \cdot \mathcal{L}_i^{c\bar{c}} + f_{B^+} \cdot \mathcal{L}_i^{B^+} + f_{B^0} \cdot \mathcal{L}_i^{B^0} + f_{\Lambda_b} \cdot \mathcal{L}_i^{l_b} \ . \quad (4)$$

The functional form of the likelihood function, $\mathcal{L}^{comb}$, used empirically to parameterize the combinatorial background, is composed of an exponential convolved with the B_s^0 boost function, $\mathcal{B}$, a fraction with no lifetime and the same double-Gaussian resolution function as the signal. This is expressed as:

$$\mathcal{L}_i^{comb}(L^i \mid \tau_{bg}, f^0, \sigma_L^i, p_{D_s}^i, s_1, s_2, f_2) =$$

$$\int_0^\infty dl \int_0^{p_{B_s}(max)} dp_{B_s} \mathcal{R}(L^i \mid l, \sigma_L^i, s_1, s_2, f_2)\mathcal{B}(p_{B_s} \mid p_{D_s}^i)\mathcal{P}_{bg}(L \mid \tau_{bg}, f^0, p_{B_s}) \ , \quad (5)$$

where the parameters describing the resolution, s_1, s_2 and f_2, are the same as used in the likelihood terms that describe the D_s^- signal and

$$\mathcal{P}_{bg}(l \mid \tau_{bg}, f^0, p_{B_s}) = (1 - f^0)\frac{m_{B_s}}{\tau_{bg} p_{B_s}} \exp\left[\frac{-l \cdot m_{B_s}}{\tau_{bg} p_{B_s}}\right] + f^0 \delta(l) \ . \quad (6)$$

The fraction of background with no lifetime, f^0, as well as the characteristic lifetime of the background, τ_{bg}, are free parameters in the fit.

The combinatorial background in the event sample is taken into account by fitting for it simultaneously with the D_s^- signal. The probability that a candidate has arisen from a combination of background tracks, $\mathcal{F}^{comb}(m_i)$, is determined as a function of the $K^+K^-\pi^-$ invariant mass of each candidate, m_i, using the results of the fit to the $K^+K^-\pi^-$ invariant mass spectrum.

Thus, the full likelihood for candidate i is:

$$\mathcal{L}_i(L^i \mid \tau_{B_s^0}, \sigma_L^i, p_{D_s}^i, m_i) = [1 - \mathcal{F}^{comb}(m_i)] \cdot \mathcal{L}_i^{D_s^-} + \mathcal{F}^{comb}(m_i) \cdot \mathcal{L}_i^{comb} \ . \quad (7)$$

In total six parameters are free in the fit: the B_s^0 lifetime, the parameters describing possible scale factors on the decay length error (s_1, s_2 and f_2) and the parameters describing the combinatorial background (f^0 and τ_{bg}).

---

[3]The D_s^- momentum dependence on The fractions $f_{c\bar{c}}$, f_{B^+}, f_{B^0} and f_{Λ_b} has been neglected. This omission was studied in simulated data and found not to produce a noticeable bias in the resulting lifetime.

The lifetime fit uses the 10633 events found in the region from 50 MeV below the fitted D_s^- mass to 200 MeV above it (see figure 1). From studies on simulated data, it is found that the lifetime properties of the combinatorial background in this region accurately reflect the combinatorial background around the D_s^- mass. Furthermore, this avoids the region below the D_s^- mass in which the number of $K^+K^-\pi^-$ candidates from D^- decays and contributions from other D meson decays (e.g. reflections and partially reconstructed decays) are potentially significant. This fit finds $\tau(B_s^0) = 1.72^{+0.20}_{-0.19}$ ps, where the error is statistical only, the values of the other free parameters of the fit are in table 3. The fitted values of the

parameter	fit results
f_2	0.07 ± 0.01
s_1	0.88 ± 0.01
s_2	4.69 ± 0.26
f^0	0.77 ± 0.01
τ_{bg}	1.61 ± 0.07

Table 3: Final values of the free parameters in the fit.

parameter are describing the decay length resolution are consistent with the understanding of the OPAL tracking performances. The decay length distributions are shown in figure 2 separately for candidates with $K^+K^-\pi^-$ invariant mass within 50 MeV of the fitted D_s^- mass (the "signal region"), and for those candidates outside this mass window (the "sideband region"). These illustrate the quality of the fit in regions dominated by D_s^- signal events and by combinatorial background, respectively. The curves in figure 2 represent the sum of the decay length probability distributions for each event. Using the 42 bins that are expected to contain at least five candidates (as predicted by the lifetime fit), a total χ^2 of 54.7 is found for the sum of the signal and sideband decay length distributions. For the positive decay length bins, a total χ^2 of 24.0 for 29 bins is observed. These χ^2 values and plots shown in figure 2 indicate that the fitted functional forms provide a good description of the data for both signal and background. It should be stressed that the fit is to the unbinned data.

5   Checks of the Method

A number of different checks have been made to investigate potential biases in the method of selecting and fitting the signal.

5.1   Potential bias in the selection and fitting procedure

Tests were performed on several samples of simulated data to check for biases in the selection and fitting procedures. The first tests involved a toy Monte Carlo program which generated decay length data for the signal D_s^- decays and combinatorial background. For each D_s^- signal candidate from a B_s^0 decay, this simulation generated B_s^0 and D_s^- decay times from exponential distributions with the means set to known values. The B_s^0 and D_s^- momenta were chosen from a spectrum based on the full Monte Carlo simulation. The B_s^0 and D_s^- decay lengths were then calculated and combined to give the true candidate decay length,
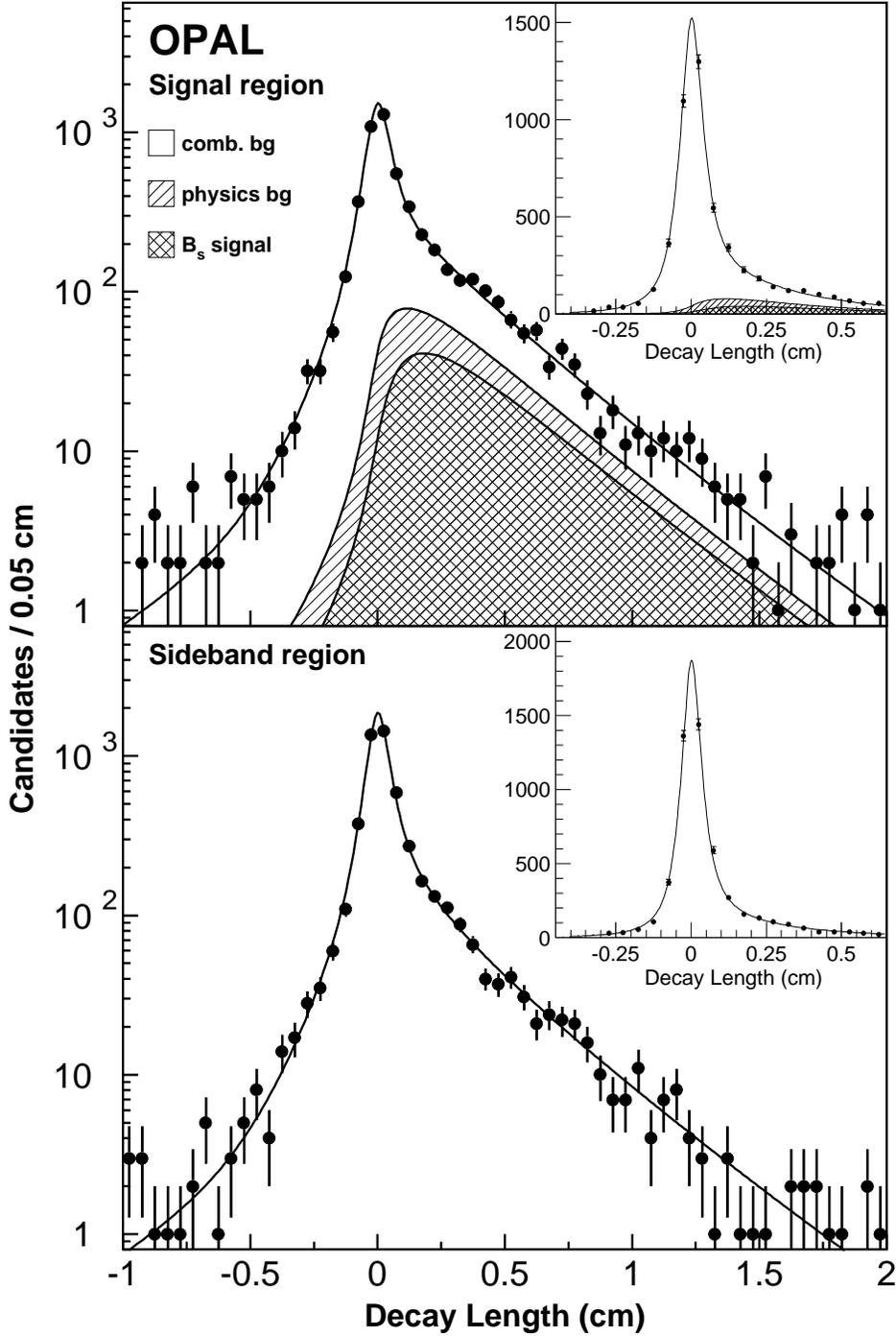
Figure 2: Top: decay length distribution within a D_s^- mass region of $\pm 50\,\text{MeV}$ around the fitted D_s^- mass (signal region). The single-hatched area represents the contribution from physics background, the unhatched area the combinatorial background and the cross-hatched area is the contribution from B_s^0 decays. Bottom: decay length distribution for events outside the D_s^- mass region (sideband region), namely from 50 to 200 MeV above the D_s^- mass.

which was then smeared by a resolution function. physics and combinatorial backgrounds were generated through a similar procedure. Many fits were conducted over wide ranges of B_s^0 lifetimes with different levels and parameterizations of the backgrounds. The result of these studies shows that any bias in the fitted B_s^0 lifetime is less than 0.5% and that the statistical precision of the fit to data is consistent with the sample size and composition.

To verify that the D_s^- selection does not bias the reconstructed sample, a lifetime measurement was made from 20000 $B_s^0 \rightarrow D_s^-$x Monte Carlo decays into the two channels of this analysis, using a B_s^0 lifetime of 1.60 ps. The mean lifetime of the selected D_s^- sample was 1.64 ± 0.04 ps, consistent with the expectation that there is no bias from the selection procedure. The lifetime obtained by fitting this same sample was 1.65 ± 0.05 ps.

To investigate the effects of the combinatorial background on the lifetime fit, the same selection and fitting procedure has been applied on a Monte Carlo sample of 4 million multihadronic z_0 decays. Due to the choice of branching ratios used to produce this sample of simulated events, there are fewer reconstructed D_s^- signal candidates than we observe in the data. The fitted lifetime has been found to be 1.73 ± 0.29 ps, which is consistent with the generated B_s^0 lifetime of 1.6 ps within the statistical power of this sample. If the signal events from the 20000 $B_s^0 \rightarrow D_s^-$x decays described above are added to the simulated data, the resulting sample is of similar purity to that found by the tight neural net selection. The fitted lifetime of this pure sample is 1.65 ± 0.07 ps, again in good agreement with the true lifetime of the sample.

The lifetime fit has also been repeated as for the standard result, except that the $\phi\pi$ and K^*K channels are fitted separately. The results are 1.53 ± 0.23 ps and 2.14 ± 0.40 ps, respectively, consistent at the level of 1.3 standard deviations.

5.2 Use of the tight (neural network) selection

As a check, a much tighter selection was developed which employs a neural network to reject significantly more combinatorial background, thereby producing a much purer D_s^- signal. However, this also results in a rather significant loss of signal, and as such is not as statistically powerful for the B_s^0 lifetime determination. This artificial neural network uses 16 kinematic and particle-identification quantities, including b-tagging information in the hemisphere opposite to the D_s^- candidate. The $K^+K^-\pi^-$ invariant mass distributions for all candidates which pass this selection are shown in figure 3. The likelihood fit to the measured $K^+K^-\pi^-$ invariant mass of the D_s^- candidates is performed as above, resulting in a smaller signal of 232 ± 29 (104 ± 17) candidates with a much reduced background fraction of $0.54(0.61)$ for the $\phi\pi$ (K^*K) mode.

The sample of D_s^- candidates found by the tighter neural network selection has also been used to fit for the B_s^0 lifetime. This sample gives a value of 1.69 ± 0.27 ps for the B_s^0 lifetime and is consistent with the more precise result from the analysis of section 4. The difference in statistical precision between the two fits is in agreement with expectation from toy Monte Carlo studies, given the relative size of the D_s^- signal and the level of combinatorial background in each sample.

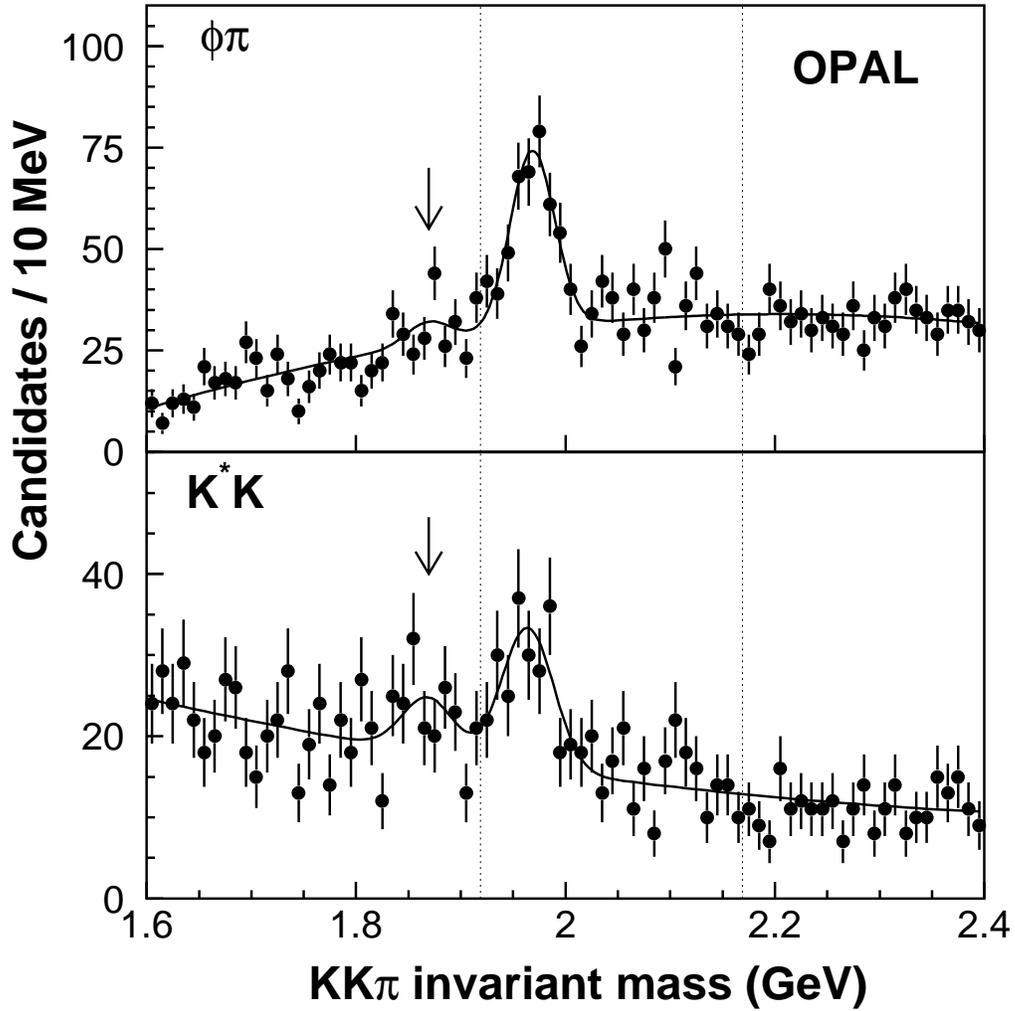The results of all of the tests show no indication of a significant bias in the selection and

Figure 3: Results of the tight (neural network) selection, used as a cross-check of the analysis. Top: $K^+K^-\pi^-$ invariant mass distribution for $\phi\pi$ combinations along with the fitted distribution. Bottom: $K^+K^-\pi^-$ invariant mass distribution for K*K candidates, along with the fitted distribution. The dotted lines indicate the region within which candidates are used in the lifetime fit for the check. The arrow indicates the d^- peak position

fitting procedures.

6   Evaluation of Systematic Errors

Systematic errors arise from the level, parameterization and source of the background, the potential bias from the selection and fitting procedure, the boost estimation method, the beam spot determination and possible tracking errors. The systematic errors are summarized in table 4.

Combinatorial background

We consider the effects of both the level of the combinatorial background, as determined by a fit to the $K^+K^-\pi^-$ mass spectrum, and the effective lifetime of this background, as estimated from the candidates in the sideband region. The systematic error due to the level of this background is determined by repeating the calculation of the event-by-event probability that an event is combinatorial background by changing the estimated size of the D_s^- signal by the statistical uncertainty from the fit to the invariant mass spectrum. This yields a variation in the B_s^0 lifetime of ± 0.08 ps. The width of the $K^+K^-\pi^-$ mass region from which candidates are selected for use in the lifetime fit has also been varied. This was done by selecting candidates in regions extending from 150 to 350 MeV above, and from 25 to 75 MeV below, the D_s^- mass. Another check included using a sideband from 200 to 350 MeV above the D_s^- mass in place of the standard sideband from 50 to 200 MeV. These change the fitted B_s^0 lifetime by ± 0.07 ps which is assigned as a systematic error. Tests were also conducted using the toy Monte Carlo which indicated that the level of these observed changes is consistent with the expected 0.05 ps uncertainty due to statistical fluctuations in the sideband sample; however we conservatively retain the observed variation as a systematic uncertainty.

Several alternative parameterizations describing of the decay length distributions of the combinatorial background have been investigated. For example, we have included an exponential on the negative decay length side, in place of the second Gaussian function, to describe those events that are significantly mis-measured. The resulting B_s^0 lifetime is $+0.02$ ps higher than the standard result. In another check the second wider Gaussian was used only for the combinatorial background term in the likelihood function, changing the lifetime by $+0.05$ ps. Leaving out this second Gaussian altogether decreased the lifetime by 0.10 ps, although the quality of this fit is significantly worse, as illustrated by an increase in χ^2 of about 300 for 40 bins, c.f. 54.7 for 42 bins with the default parameterization. Consequently this last case is not considered as a systematic error. In no case do these alternative parameterizations significantly improve the quality of the B_s^0 lifetime fit, and an error of ± 0.05 ps was assigned to cover such effects.

We assign a total systematic error due to the combinatorial background, parameterization and source, of ± 0.12 ps.

Physics background: sources of D_s^- mesons

The physics background composition has already been discussed. Varying the fraction of D_s^- mesons from $Z^0 \to c\bar{c}$ events over the range given in Table 2 produces a change of $^{+0.12}_{-0.11}$ ps

in the B_s^0 lifetime. The uncertainty due to the D_s^- fraction from b-hadrons other than B_s^0 is evaluated in the same way. The observed change on the B_s^0 lifetime is $^{+0.04}_{-0.03}$ ps. These variations also change the statistical error on the fitted B_s^0 lifetime by up to ± 0.03 ps, and this systematic effect is not considered further.

The B_s^0 lifetime dependence on the uncertainty of the b-hadron lifetimes has been measured by varying the b-hadron lifetimes within the errors quoted in reference [1], assuming, conservatively, that the individual lifetimes are fully correlated with each other. The B_s^0 lifetime changed by ± 0.02 ps, which is included as a systematic error. The D_s^- lifetime has also been varied in the fit, within the errors quoted in reference [1]. The effect on the measured B_s^0 lifetime is ± 0.01 ps. This variation is also taken as a contribution to the systematic error.

The D_s^- momentum spectrum also depends on the fragmentation in $Z^0 \to c\bar{c}$ and $Z^0 \to b\bar{b}$ events. Changes in the fragmentation affect the composition of the D_s^- signal through changes in the efficiencies for the charm and bottom contributions to the D_s^- signal (the effect of the momentum spectrum of the D_s^- in $Z^0 \to b\bar{b}$ events on the estimation of the B_s^0 momentum in the lifetime fit is discussed below). In $Z^0 \to b\bar{b}$ events, we have varied the average b hadron energy by the measurement errors [15] to yield a variation in the observed lifetime of ± 0.01 ps. Similarly, the momenta of the D_s^- mesons produced in $Z^0 \to c\bar{c}$ events was varied according to the average energy measured for non-strange mesons in $Z^0 \to c\bar{c}$ events (on the assumption that there is little difference in fragmentation amongst the various charm mesons) [14], producing a variation of ± 0.01 ps in $\tau(B_s^0)$.

In the case of D_s^- mesons coming from the decay of b-hadrons other than B_s^0, the D_s^- may be produced in either a two-body mode (e.g. $B \to D_s^- D$) or a multi-body final state where one or more light particles are produced. The two-body decay fraction of $B \to D_s^- X$ has been measured to be 0.56 ± 0.10 [16]. In determining the relative efficiency of these D_s^- mesons from b-hadrons other than B_s^0, we have already corrected our simulation to this two-body fraction. Assuming b-baryons decaying to D_s^- mesons in two- or multi-body states have the same fractions as B^+ and B^0 mesons, the efficiency of selecting D_s^- mesons from these decays has been evaluated by varying the two-body fraction over the range 0.46 to 0.66 and re-evaluating the relative efficiency of this source of D_s^- with respect to the D_s^- which arise from a B_s^0 decay. This produces a variation of ± 0.01 ps in the fitted B_s^0 lifetime.

Thus we assign a total error due to these other sources of D_s^- mesons of $^{+0.13}_{-0.12}$ ps.

Boost estimation

The energy spectrum of the Monte Carlo B_s^0 events used to estimate the momentum of the B_s^0, given the observed D_s^- momentum, can also affect the resulting lifetime. This effect is not large because the scaling used to estimate the B_s^0 momentum from the measured D_s^- momentum is correlated with the D_s^- momentum itself. We have varied the average B_s^0 energy by the measured errors on the average b-hadron energy [15] to yield a variation in the B_s^0 lifetime of ± 0.01 ps.[4] The effect of a 2.0 MeV uncertainty in the mass of the B_s^0 [1] was found to produce a change of less than 0.01 ps in the B_s^0 lifetime.

---

[4]Note that the uncertainty due to the bottom and charm hadron energy spectra affects the B_s^0 lifetime both through the boost estimation and through the D_s^- sample composition. When combined, these two contributions are added linearly.

Beam position and size

The average intersection point of the LEP beams in OPAL is used to estimate the production vertex of the B_s^0 candidates. The sensitivity of $\tau(B_s^0)$ to the assumed position and size of the beam spot has been evaluated as in reference [6], resulting in a variation in the fitted lifetime of no more than 0.01 ps, which has been assigned as a systematic error.

Detector alignment

The effects of alignment and calibration uncertainties on the B_s^0 lifetime are estimated from a detailed study of 3-prong τ decays [13]. These uncertainties lead to an uncertainty of 0.01 ps on $\tau(B_s^0)$.

source	uncertainty (ps)
combinatorial background	± 0.12
physics background	$^{+0.13}_{-0.12}$
uncertainty in boost	± 0.01
beam spot	± 0.01
alignment errors	± 0.01
total	$^{+0.18}_{-0.17}$

Table 4: Summary of systematic errors on the B_s^0 lifetime.

Combining the systematic errors in Table 4, we find $\tau(B_s^0) = 1.72^{+0.20}_{-0.19}(\text{stat})^{+0.18}_{-0.17}(\text{syst})$ ps.

7 Conclusion

A sample of D_s^- decays has been reconstructed in which the D_s^- has decayed into $K^+K^-\pi^-$ through either the $\phi\pi^-$ or $K^{*0}K^-$ channels. From 3.7 million hadronic Z^0 events recorded by OPAL from 1991 to 1995, a total of 911 ± 83 such candidate decays have been found, of which about 57% are expected to be from B_s^0 decay. The B_s^0 lifetime is found to be

$$\tau(B_s^0) = 1.72^{+0.20}_{-0.19}(\text{stat})^{+0.18}_{-0.17}(\text{syst}) \text{ ps},$$

a result consistent with the measured B^0 lifetime and other B_s^0 measurements [1]. This result is also in agreement with current theoretical expectations [3, 4].

References

[1] Particle Data Group, R.M. Barnett et al., Phys. Rev. **D 54** (1996) 1.

[2] G. Altarelli and S. Petrarca, Phys. Lett. **B 261** (1991) 303;
I.I. Bigi, Phys. Lett. **B 169** (1986) 101;
J.H. Kühn et al., *Heavy Flavours at LEP*, MPI–PAE/PTh 49/89, August 1989, contribution
by R. Rückl, p. 59.

[3] I. Bigi, Nuovo Cim. **109A** (1996) 713;
I. Bigi et al., (CERN-TH.7132/94), from the second edition of the book 'B Decays,' S. Stone
(ed.), World Scientific, pp. 132-157;
I. Bigi and N.G. Uraltsev, Phys. Lett. **B 280** (1992) 271.

[4] M. Neubert, C.T. Sachrajda, Nucl. Phys. **B483** (1997) 339.

[5] ALEPH Collab., D. Buskulic et al., Phys. Lett. **B377** (1996) 205;
ALEPH Collab., D. Buskulic et al., Zeit. Phys, **C69** (1996) 585;
CDF Collab., F. Abe et al., Phys. Rev. Lett. **77** (1996) 1945;
CDF Collab., F. Abe et al., Phys. Rev. Lett. **74** (1995) 4988;
DELPHI Collab., P. Abreu et al., Zeit. Phys. **C71** (1996) 11.

[6] OPAL Collab., R.Akers et al., Phys. Lett. **B350** (1995) 273 .

[7] OPAL Collab., K. Ahmet et al., Nucl. Inst. and Meth. **A 305** (1991) 275;
P.P. Allport et al., Nucl. Inst. and Meth. **A 324** (1993) 34;
P.P. Allport et al., Nucl. Inst. and Meth. **A 346** (1994) 479.

[8] O. Biebel et al., Nucl. Inst. and Meth. **A 323** (1992) 169;
M. Hauschild et al., Nucl. Inst. and Meth. **A 314** (1992) 74.

[9] OPAL Collab., G. Alexander et al., Z. Phys. **C 52** (1991) 175.

[10] JADE Collab., W. Bartel et al., Z. Phys. **C 33** (1986) 23;
JADE collab., S. Bethke et al., Phys. Lett. **B 213** (1988) 235.

[11] T. Sjöstrand, Comp. Phys. Comm. **82** (1994) 74.
The OPAL parameter optimization is described in
OPAL Collab., G, Alexander et al., Z. Phys. **C 69** (1996) 543.

[12] J. Allison et al., Nucl. Inst. and Meth. **A 317** (1992) 47.

[13] OPAL Collab., P.D. Acton et al., Z. Phys. **C 59** (1993) 183;
OPAL Collab., R. Akers et al., Phys. Lett. **B 338** (1994) 497.

[14] OPAL Collab., G. Alexander et al., Z. Phys. **C 72** (1996) 1.

[15] The LEP Collaborations, ALEPH, DELPHI, L3 and OPAL, and the LEP Electroweak working
group, CERN-PPE/96-017, accepted by Nuclear Instruments and Methods.

[16] ARGUS Collab., H. Albrecht et al., Z. Phys. **C 54** (1992) 1;
CLEO Collab., D. Bortoletto et al., Phys. Rev. **D 45** (1992) 21;
CLEO Collab., D. Bortoletto et al., Phys. Rev. Lett. **64** (1990) 2117.